Multiclass Flight Anomaly Detection Using Dempster-Shafer Theoretic Sensor Fusion

AIAA SciTech Forum 2024 @ Orlando, FL

Ezequiel Juarez Garcia[1], Szilard L. Beres[1], Markus L. Mulvihill[1], Chad L. Stephens[2], and Nicholas J. Napoli[1]

January 12, 2024

[1]Human Informatics and Predictive Performance Optimization (**HIPPO**) Laboratory
[2]NASA Crew Systems & Aviation Operations Branch and System-Wide Safety Project

UF Herbert Wertheim College of Engineering
UNIVERSITY of FLORIDA

Bottom Line Up Front

- Rise in complexity of aviation systems[1] has resulted in complex methods for detecting high-risk events/anomalies
- We propose a method to capture the multivariate state of the system and predict anomalies using Dempster-Shafer Theoretic (DST) sensor fusion
- Our methodology shows an improvement in classification performance compared to majority voting

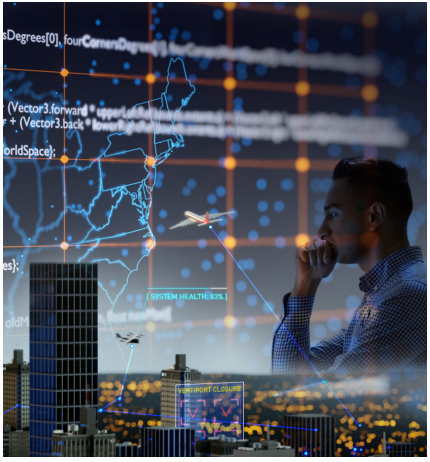

Image courtesy of NASA

Motivation

Image courtesy of John McArthur on Unsplash.

- Modern safety programs seek to safeguard against current *and* future risks
- Ahead-of-time identification of anomalies can increase time for corrective action
- Data-driven methods should be fundamentally interpretable and capable of generalizing to future airframes

Prior Work

- Traditional anomaly detection relies on threshold exceedance.
- New deep learning approaches have shown success in detecting known anomalies[2].
  - Lack interpretability $\rightarrow$ **lack of understanding of driving factors & inadequate time for remediation**.
- Our previous work provided predictive analysis of unstable approaches[3].
  - Simple model was able to provide good classification performance
  - Can benefit from more sensors

Image courtesy of Flight Safety Foundation.

Challenges and Insights

Challenges

1. Rise in system complexity has resulted in more complex patterns of failure
2. Poor end-user interpretability is a barrier for certification

Insights

1. Capture the multivariate aircraft dynamics using interpretable features
2. Use sensor fusion to combine information from multiple models for improved accuracy and interpretability

Methods: Dataset Overview

- The NASA DASHlink Sample Flight Data contains 180,000 commercial flights[4]
- Each flight has over 180 flight variables
- Last 160 seconds before touchdown were analyzed
- Anomalies were identified after the 1,000 ft height above ground level (AGL) crossing

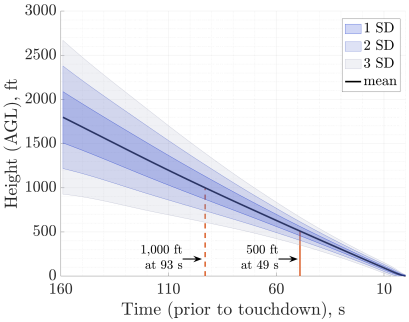

Anomaly	Threshold
High speed	Difference in airspeed and setpoint 2 SD above nominal
High path	Height AGL 2 SD above nominal at same point in time
Late flaps setting	Flaps deployed 60 seconds later than nominal

Methods: Ordinal Patterns

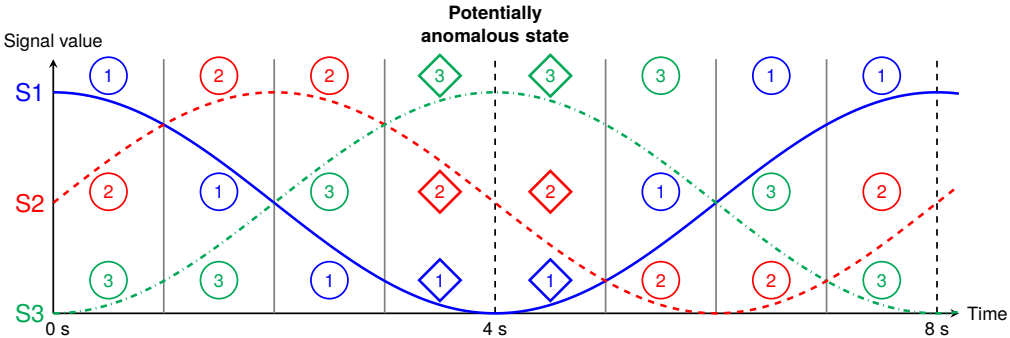

- Ordinal patterns capture how signals are ranked, or ordered, at any point in time.
- Each pattern can be treated as a state. For example, state 1 can be pattern (3, 2, 1).

Methods: Time Series Normalization

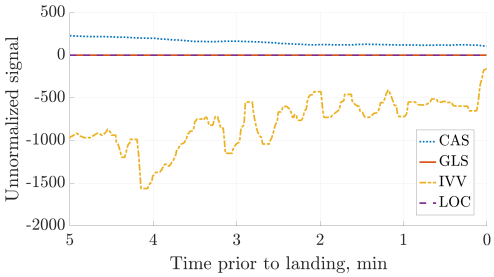

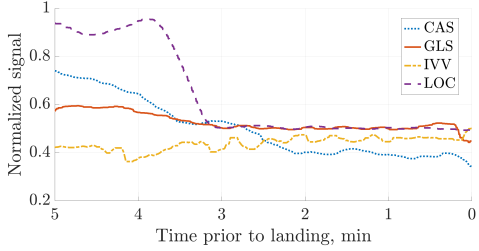

- CAS = airspeed
- GLS = glideslope deviation
- IVV = vertical velocity
- LOC = localizer deviation

Methods: Sensor Fusion

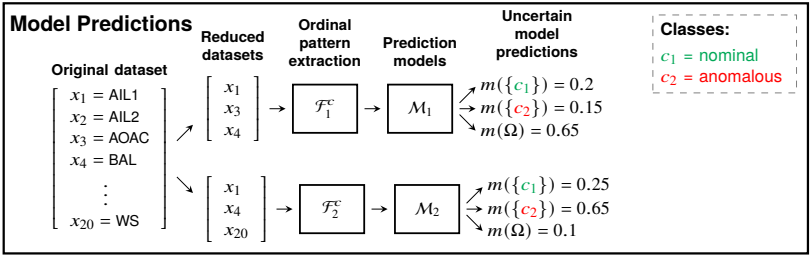

See Appendix B for complete list of flight variables

Results: Research Questions (RQs)

RQ1 What is the prediction performance increase when using Dempster-Shafer Theoretic (DST) fusion compared to a more traditional majority vote approach?

RQ2 How can the variable combinations help us identify the ordinal patterns closely linked to anomalies?

Results: RQ1) Performance Increase of DST Fusion

Results at 100 s before landing with [left] no fusion (NF) and [right] DST fusion (DSF)

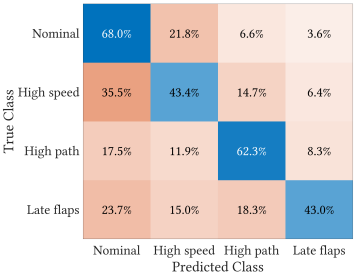

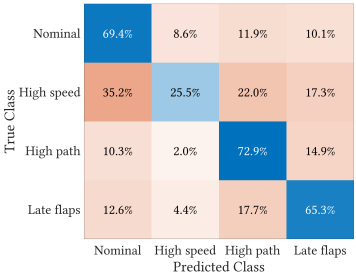

Performance Metric	Class	Time Prior to Landing							
		160 s		140 s		120 s		100 s	
		NF	DSF	NF	DSF	NF	DSF	NF	DSF
MCC	(Overall)	0.20	0.22	0.26	0.29	0.32	0.36	0.39	0.45
F1 Score	(Overall)	0.39	0.41	0.44	0.46	0.48	0.51	0.54	0.58

Takeaway: The increased detection performance of minority classes can help identify rare anomaly occurrences.

Results: Research Questions (RQs)

RQ1 What is the prediction performance increase when using Dempster-Shafer Theoretic (DST) fusion compared to a more traditional majority vote approach?

RQ2 How can the variable combinations help us identify the ordinal patterns closely linked to anomalies?

Results: RQ2) Ordinal Patterns Linked to Anomalies

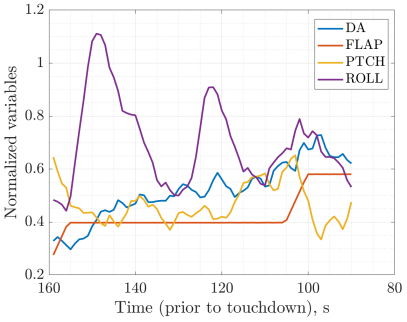

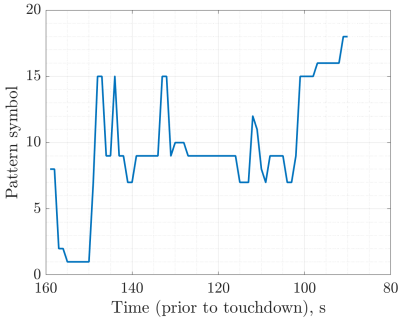

DA = drift angle, FLAP = flap position, PTCH = pitch angle, ROLL = roll angle

Results: RQ2) Ordinal Patterns Linked to Anomalies

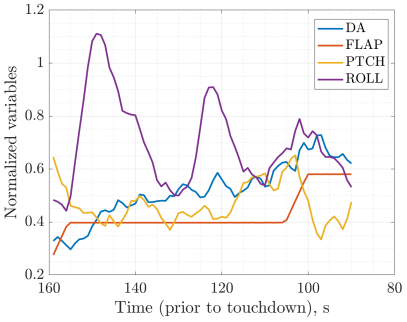

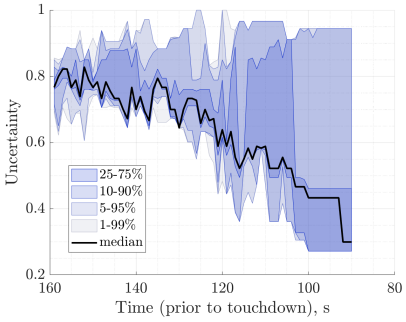

DA = drift angle, FLAP = flap position, PTCH = pitch angle, ROLL = roll angle

Takeaway: The decreasing uncertainty as we get closer to landing reflects the increased performance of our anomaly detection methodology.

Conclusion and Future Work

- We provide a more interpretable approach to predict in-flight anomalies
- We observe an improvement in classification performance over majority voting
- The classification performance can be improved through the
  - Extended use of Dempster-Shafer theory to sets with more than one class
  - Increased number of flight variables per combination
  - Testing on imbalanced dataset
  - Comparison to recent research advances

Image courtesy of NASA.

References

[1] P. S. Oliveira Filho, “The growing level of aircraft systems complexity and software investigation,” [Online], International Society of Air Safety Investigators, 2018. [Online]. Available: https://www.isasi.org/Documents/library/technical-papers/2018/Wed/The%20Growing%20Level%20of%20Aircraft%20Systems%20Complexity%20and%20Software%20Investigation%20-%20Paulo%20Soares%20Oliveria%20Filho.pdf

[2] L. Basora, X. Olive, and T. Dubot, “Recent Advances in Anomaly Detection Methods Applied to Aviation,” *Aerospace*, vol. 6, no. 11, p. 117, Nov. 2019.

[3] E. Juarez Garcia, M. L. Mulvihill, M. S. Kharab, C. L. Stephens, and N. J. Napoli, “Capturing Multivariate Time Series Interactions to Detect High-Risk Instability During Approach,” in *AIAA AVIATION 2023 Forum*. San Diego, CA: American Institute of Aeronautics and Astronautics, 2023.

[4] NASA, “DASHlink – Sample Flight Data,” NASA, 2012. [Online]. Available: https://c3.ndc.nasa.gov/dashlink/projects/85/

Contact Information and Funding

- Ezequiel Juarez Garcia (ejuarezgarcia@ufl.edu)
- Chad L. Stephens (chad.l.stephens@nasa.gov)
- Nicholas J. Napoli (n.napoli@ufl.edu)

This work was funded by **NASA**.

Thank you.
Questions?

HIPPO Lab Website

https://hippo.ece.ufl.edu/

Appendix A: All Performance Metrics

Performance Metric	Class	Time Prior to Landing							
		160 s		140 s		120 s		100 s	
		NF	DSF	NF	DSF	NF	DSF	NF	DSF
BA	Nominal	0.65	0.66	0.69	0.72	0.72	0.75	0.71	0.75
	High speed	0.50	0.51	0.54	0.55	0.54	0.54	0.64	0.60
	High path	0.64	0.65	0.65	0.66	0.69	0.70	0.75	0.78
	Late flaps	0.58	0.60	0.62	0.63	0.67	0.71	0.68	0.76
MCC	Nominal	0.27	0.29	0.33	0.39	0.39	0.44	0.38	0.47
	High speed	0.02	0.05	0.13	0.16	0.12	0.14	0.28	0.29
	High path	0.25	0.27	0.29	0.30	0.37	0.38	0.49	0.52
	Late flaps	0.18	0.20	0.26	0.27	0.35	0.41	0.44	0.50
F1 Score	Nominal	0.48	0.49	0.53	0.56	0.57	0.60	0.56	0.61
	High speed	0.08	0.09	0.19	0.22	0.22	0.22	0.45	0.36
	High path	0.47	0.48	0.48	0.49	0.53	0.55	0.62	0.65
	Late flaps	0.36	0.39	0.42	0.45	0.50	0.56	0.53	0.63
MCC	(Overall)	0.20	0.22	0.26	0.29	0.32	0.36	0.39	0.45
F1 Score	(Overall)	0.39	0.41	0.44	0.46	0.48	0.51	0.54	0.58

Appendix B: Variable Descriptions

Index/Symbol	Variable Description	Identifier/Name	Unit
1	Left aileron position	AIL1	degree
2	Right aileron position	AIL2	degree
3	Angle of attack	AOAC	degree
4	Altitude (baro corrected)	BAL	feet
5	Airspeed	CAS	knots
6	Selected course angle	CRSS	degree
7	Drift angle	DA	degree
8	Left elevator position	ELEV1	degree
9	Flap position	FLAP	discrete count
10	Glideslope deviation	GLS	percentage
11	Selected heading angle	HDGS	degree
12	Localizer deviation	LOC	percentage
13	Core average speed (engine)	N2	percentage
14	Total pressure	PT	mbar
15	Pitch angle	PTCH	degree
16	Roll angle	ROLL	degree
17	Rudder position	RUDD	degree
18	True heading angle	TH	degree
19	Vertical acceleration	VRTG	g (m/s^2)
20	Wind speed	WS	knots
21	Selected airspeed	CASS	knots

Appendix C: Variable Combinations

Combination	Fold 1	Fold 2	Fold 3	Fold 4	Fold 5
1	9, 10, 15, 20	7, 9, 10, 20	3, 7, 12, 20	4, 7, 10, 15	7, 10, 12, 16
2	4, 7, 10, 12	10, 14, 15, 16	7, 10, 12, 14	12, 13, 14, 15	10, 13, 15, 16
3	7, 15, 16, 20	3, 9, 10, 16	7, 10, 16, 20	7, 9, 15, 20	7, 12, 14, 16
4	3, 7, 12, 13	3, 7, 9, 20	7, 9, 12, 15	9, 10, 15, 16	7, 10, 12, 13
5	10, 12, 16, 20	7, 12, 13, 15	3, 9, 10, 20	7, 12, 13, 16	3, 7, 12, 16
6	3, 7, 16, 20	7, 12, 13, 20	7, 9, 16, 20	7, 13, 15, 20	7, 9, 12, 20
7	9, 10, 12, 20	3, 7, 13, 20	5, 7, 10, 16	12, 14, 15, 16	9, 15, 16, 20
8	3, 9, 12, 20	10, 12, 13, 20	12, 15, 16, 20	3, 7, 9, 12	7, 12, 14, 15
9	3, 12, 13, 16	3, 13, 16, 20	10, 12, 13, 15	7, 10, 12, 20	10, 13, 14, 16
10	7, 12, 15, 20	7, 9, 10, 15	10, 12, 14, 15	9, 10, 16, 20	10, 13, 16, 20
11	10, 12, 15, 16	7, 10, 14, 15	7, 9, 15, 16	10, 12, 14, 16	7, 10, 13, 20
12	4, 10, 15, 16	9, 10, 12, 16	3, 10, 13, 20	7, 9, 10, 12	3, 7, 13, 16
13	3, 7, 9, 10	3, 12, 16, 20	4, 7, 10, 16	4, 7, 12, 15	12, 13, 15, 20
14	3, 7, 9, 16	7, 10, 15, 16	9, 10, 12, 15	7, 10, 14, 16	3, 9, 16, 20
15	7, 10, 15, 20	7, 12, 13, 14	13, 15, 16, 20	3, 7, 10, 16	12, 13, 14, 16
16	4, 12, 15, 16	10, 13, 14, 15	10, 12, 15, 20	3, 10, 16, 20	3, 10, 12, 13
17	10, 12, 13, 14	3, 9, 12, 16	7, 13, 14, 15	7, 10, 12, 15	3, 7, 10, 13
18	7, 13, 15, 16	3, 7, 10, 12	4, 10, 12, 16	5, 10, 12, 16	5, 7, 12, 16
19	7, 10, 13, 16	3, 10, 12, 20	7, 10, 13, 14	13, 14, 15, 16	3, 9, 10, 12
20	7, 10, 13, 15	12, 13, 16, 20	3, 7, 10, 20	7, 12, 15, 16	9, 12, 15, 16

Appendix D: Pattern to Symbol Mapping

Pattern	Symbol	Pattern	Symbol
(a, b, c, d)	1	(c, a, b, d)	13
(a, b, d, c)	2	(c, a, d, b)	14
(a, c, b, d)	3	(c, b, a, d)	15
(a, c, d, b)	4	(c, b, d, a)	16
(a, d, b, c)	5	(c, d, a, b)	17
(a, d, c, b)	6	(c, d, b, a)	18
(b, a, c, d)	7	(d, a, b, c)	19
(b, a, d, c)	8	(d, a, c, b)	20
(b, c, a, d)	9	(d, b, a, c)	21
(b, c, d, a)	10	(d, b, c, a)	22
(b, d, a, c)	11	(d, c, a, b)	23
(b, d, c, a)	12	(d, c, b, a)	24